

SCIENTIFIC REPORTS



OPEN

Pioglitazone Ameliorates Smooth Muscle Cell Proliferation in Cuff-Induced Neointimal Formation by Both Adiponectin-Dependent and -Independent Pathways

Tetsuya Kubota^{1,2,3,4,*}, Naoto Kubota^{1,2,3,5,*}, Hiroyuki Sato^{1,*}, Mariko Inoue^{1,3}, Hiroki Kumagai¹, Tomokatsu Iwamura¹, Iseki Takamoto¹, Tsuneo Kobayashi⁶, Masao Moroi⁴, Yasuo Terauchi⁷, Kazuyuki Tobe⁸, Kohjiro Ueki¹ & Takashi Kadowaki¹

The aim of this study is to elucidate to what degree adiponectin is involved in TZD-mediated amelioration of neointimal formation. We investigated the effect of 3- or 8-weeks' pioglitazone on cuff-induced neointimal formation in adiponectin-deficient (APN-KO) and wild-type (WT) mice. Pioglitazone for 3 weeks reduced neointimal formation in the WT mice with upregulation of the plasma adiponectin levels, but failed to reduce neointimal formation in the APN-KO mice, suggesting that pioglitazone suppressed neointimal formation by adiponectin-dependent mechanisms. Pioglitazone for 3 weeks suppressed vascular smooth muscle cell (VSMC) proliferation and increased AdipoR2 expression in the WT mice. *In vitro*, globular adiponectin activated AMPK through both AdipoR1 and AdipoR2, resulting in the inhibition of VSMC proliferation. Interestingly, 8-weeks' pioglitazone was reduced neointimal formation in APN-KO mice to degree similar to that seen in the WT mice, suggesting that pioglitazone can also suppress neointimal formation via a mechanism independent of adiponectin. Pioglitazone for 8 weeks completely abrogated the increased VSMC proliferation, along with a reduction of cyclin B1 and cyclin D1 expressions and cardiovascular risk profile in the APN-KO mice. *In vitro*, pioglitazone suppressed these expressions, leading to inhibition of VSMC proliferation. Pioglitazone suppresses neointimal formation via both adiponectin-dependent and adiponectin-independent mechanisms.

Thiazolidinediones (TZDs) have been shown to act as insulin sensitizers in both animals and humans with obesity-linked insulin resistance and type 2 diabetes^{1–4}, and are used as one class of therapeutic agents in the treatment of type 2 diabetes mellitus. In addition to controlling glycemia, TZDs have also been shown to have beneficial effects on other cardiovascular risk factors, such as dyslipidemia and hypertension⁵. Moreover, TZDs have been demonstrated to suppress atherosclerosis independent of their effects on these risk factors^{6–10}, suggesting that TZDs may have direct actions on the vasculature. A previous meta-analysis indicated that TZDs reduced the risk of repeat revascularization in patients undergoing percutaneous coronary intervention (PCI)¹¹. Pioglitazone, one of the representative TZDs, was shown in a PRO active study to reduce the composite of all-cause mortality,

¹Department of Diabetes and Metabolic Diseases, Graduate School of Medicine, University of Tokyo, Tokyo 113-8655, Japan. ²Laboratory for Metabolic Homeostasis, RIKEN Center for Integrative Medical Sciences, Kanagawa, 230-0045, Japan. ³Department of Clinical Nutrition, National Institute of Health and Nutrition, Tokyo 162-8636, Japan. ⁴Division of Cardiovascular Medicine, Toho University Ohashi Medical Center, Tokyo 153-8515, Japan. ⁵Department of Clinical Nutrition Therapy, University of Tokyo, Tokyo 113-8655, Japan. ⁶Department of Physiology and Morphology, Institute of Medicinal Chemistry, Hoshi University, Tokyo 142-8501, Japan. ⁷Department of Diabetes and Endocrinology, Yokohama City University, School of Medicine, Kanagawa 236-0004, Japan. ⁸First Department of Internal Medicine, Faculty of Medicine, University of Toyama, Toyama, 930-0194, Japan. *These authors contributed equally to this work. Correspondence and requests for materials should be addressed to N.K. (email: nkubota-tky@umin.ac.jp) or T. Kadowaki (email: kadowaki-3im@h.u-tokyo.ac.jp)

non-fatal myocardial infarction and stroke in patients with type 2 diabetes who are at a high risk of developing macrovascular events¹².

TZDs activate peroxisome proliferator-activated receptor gamma (PPAR γ), which is a member of the nuclear hormone receptor superfamily, and is expressed on major cells involved in the development of atherosclerosis, including endothelial cells, vascular smooth muscle cells (VSMCs) and monocytes/macrophages^{13–15}. Pioglitazone failed to attenuate the massive vascular lesion formation in the transplanted carotid artery from VSMC-specific PPAR γ -deficient mice¹⁶. Pioglitazone also failed to suppress atherosclerosis in SMC-specific PPAR γ /low-density lipoprotein receptor (LDLR) double-deficient mice¹⁷. A recent study revealed that pioglitazone modulated VSMC proliferation via PPAR γ ¹⁸. These data suggest that pioglitazone suppresses atherosclerosis through the PPAR γ expressed in VSMCs.

In addition to the direct vascular effects of TZDs, TZDs have been shown to upregulate adiponectin expression in white adipose tissue and to increase the plasma adiponectin levels, which is well known to have anti-atherogenic properties¹⁹. We and others have previously demonstrated that adiponectin-deficient (APN-KO) mice show neointimal formation in response to cuff- or wire-injury, and that adenovirus vector-mediated adiponectin transfection suppressed the VSMC proliferation and migration^{20–22}. Many epidemiological studies have revealed a relationship between plasma adiponectin levels and the risk of cardiovascular events^{23,24}. Moreover, two distinct adiponectin receptors have been identified: AdipoR1 and AdipoR2²⁵. Although AdipoR1 and AdipoR2 expression levels show tissue-specific differences, both are expressed in the vasculature, including the VSMCs and endothelial cells. The expression levels of AdipoR1 and AdipoR2 have been shown to be significantly reduced in the coronary arteries of animal models of type 2 diabetes²⁶. These findings suggest that the anti-atherogenic actions of TZDs are adiponectin-dependent. However, whether the TZD-induced increase in plasma adiponectin is causally involved in the anti-atherogenic effects of TZDs has not yet been addressed.

In the present study, we used APN-KO mice to investigate whether pioglitazone, one of the representative TZDs, is capable of ameliorating neointimal formation in the absence of adiponectin. In the wild-type (WT) mice, pioglitazone treatment was associated with a significant increase of the plasma adiponectin from 1 week onward, and 3-weeks' treatment was associated with attenuation of cuff-induced neointimal formation. On the other hand, in the APN-KO mice, the cuff-induced neointimal formation remained unchanged after 3 weeks of pioglitazone treatment, suggesting that the pioglitazone-induced suppression of cuff-induced neointimal formation in the WT mice was dependent on adiponectin. Cuff-induced neointimal formation is associated with the proliferation of α -smooth muscle actin-positive cells, and the VSMC proliferation was significantly suppressed after 3-weeks' pioglitazone treatment in the WT mice, but not APN-KO mice. Moreover, increased AdipoR2 expression levels were observed in the neointima after 3-weeks' pioglitazone treatment, suggesting that this upregulation is augmented adiponectin's action. Adiponectin attenuated the VSMC proliferation induced by platelet-derived growth factor (PDGF)-BB through the AdipoR1- and AdipoR2- AMPK pathways in human aortic SMCs (HASMCs). Interestingly, however, both WT and APN-KO mice exhibited similar significant improvement of neointimal formation after 8-weeks' pioglitazone treatment, associated with a reduction of the cardiovascular risk profile. These data suggest that pioglitazone can also suppress neointimal formation independently of its actions mediated by adiponectin. The increased VSMC proliferation in the APN-KO mice was completely reversed after 8 weeks of pioglitazone treatment, along with a reduction of cyclinB1 and cyclinD1 expression levels. Pioglitazone directly inhibited VSMC proliferation via suppression of these expression levels in HASMCs. Taken together, pioglitazone-induced amelioration of neointimal formation may occur via both adiponectin-dependent and adiponectin-independent mechanisms.

Results

Pioglitazone treatment for 3 weeks suppressed neointimal formation induced by cuff injury in an adiponectin-dependent manner, accompanied by augmentation of AdipoR2 expression.

Significant increase of the plasma total adiponectin levels was observed from 1 week onward after the start of pioglitazone treatment in the WT mice, but not APN-KO mice (Fig. 1a). Furthermore, increased plasma high-molecular-weight (HMW) adiponectin levels were also observed from 1 week after the start of pioglitazone treatment in the WT mice, but not in the APN-KO mice (Supplementary Fig. S1). To investigate whether this increase of the plasma adiponectin was associated with suppression of neointimal formation, cuff injury was induced in the femoral artery of the WT and APN-KO mice during 3 weeks the course of pioglitazone treatment. The APN-KO mice showed a significant cuff-induced increase of the intimal thickness and intimal/medial volume ratio (Fig. 1b,c,g,i), as previously reported²⁰. Pioglitazone treatment for 3 weeks significantly reduced the intimal thickness and intimal/medial volume ratio in the WT mice, but not in the APN-KO mice (Fig. 1d,e,g,i). No significant differences were observed in the mean diameter or medial thickness among the WT and APN-KO mice either before and after pioglitazone treatment (Fig. 1f,h). Since PPAR γ agonists have been reported to upregulate AdipoR2 mRNA expression, we next investigated the expression levels of AdipoR1 and AdipoR2 mRNA in the cuff-induced neointimal formation after 3 weeks of pioglitazone treatment. Although the AdipoR1 mRNA expression levels did not differ among the four groups, pioglitazone treatment for 3 weeks was associated with increased AdipoR2 mRNA expression levels in the cuff-induced neointimal formation in both the WT and APN-KO mice (Fig. 1j). Increase of the AdipoR2 mRNA expression level was also observed in the endothelium-denuded aorta of both WT and APN-KO mice after 3 weeks of pioglitazone treatment (Fig. 1k). These data suggest that 3 weeks of pioglitazone treatment suppressed neointimal formation in an adiponectin-dependent manner, accompanied by augmentation of AdipoR2 expression.

Pioglitazone treatment inhibited VSMC proliferation in the cuff-induced neointimal formation in an adiponectin-dependent manner. The neointimal thickness was next assessed by α -smooth muscle actin staining. The majority of cells in the neointima of the cuff-injured vessels, as well as in the media, showed

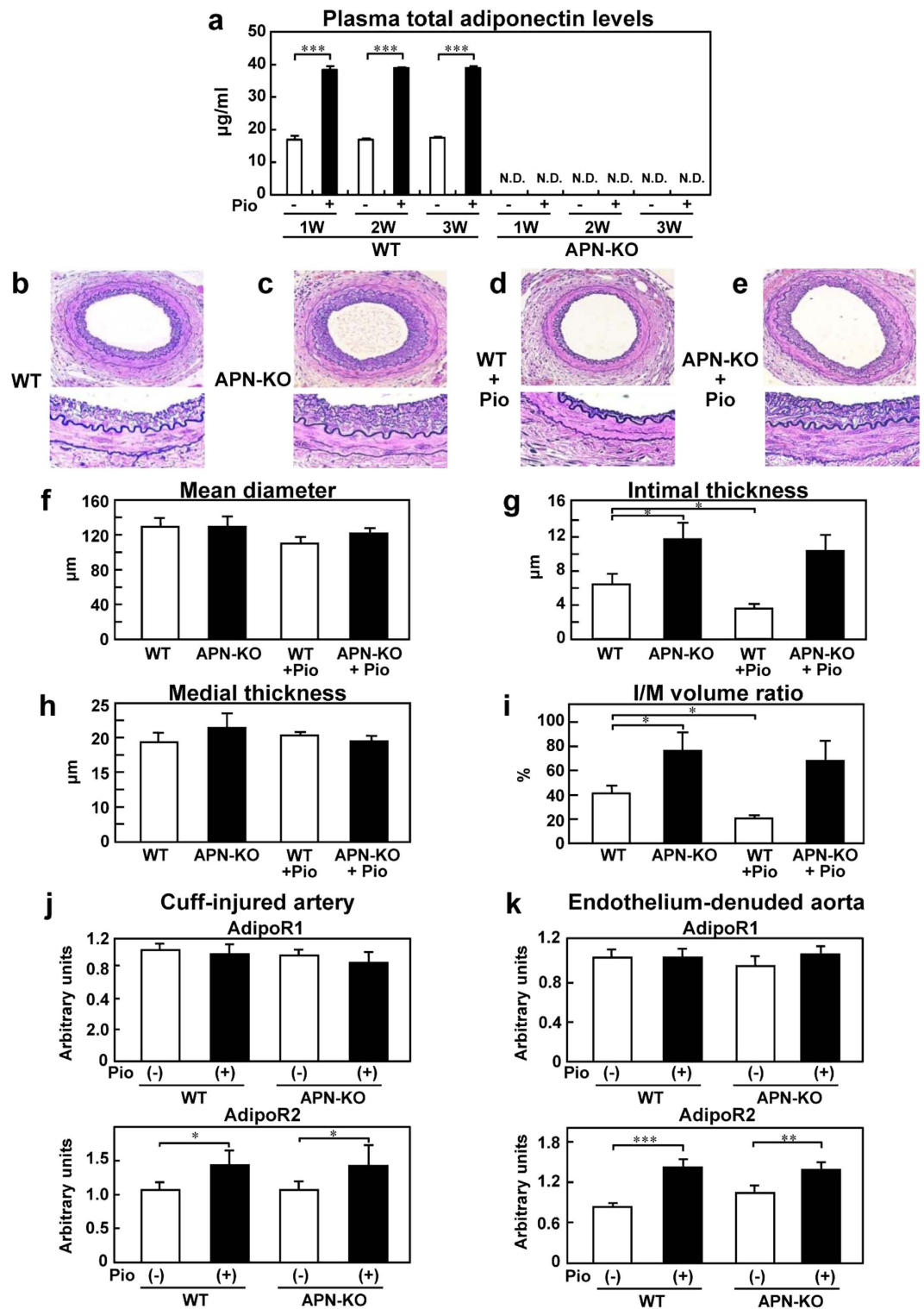


Figure 1. Pioglitazone treatment for 3 weeks inhibited cuff-induced neointimal formation in the WT, but not APN-KO mice. (a) Plasma total adiponectin levels after 3 weeks of treatment with pioglitazone in the WT and APN-KO mice (n = 5). Representative cuff-injured vessels from WT (b) APN-KO (c) WT+pioglitazone (Pio) (d) and APN-KO+Pio (e) mice after 3-weeks' pioglitazone treatment (upper; $\times 40$, lower; $\times 400$). Morphometric analysis of the blood vessels in the WT and APN-KO mice; Mean diameter (f), Intimal thickness (g) Medial thickness (h) Intima-to-media (I/M) volume ratio (i) in response to vessel injury after 3-weeks' treatment with pioglitazone (n = 8–12). Expression levels of AdipoR1 and AdipoR2 in the cuff-injured artery (j) and endothelium-denuded aorta (k) in the WT and APN-KO mice (n = 5–8). N.D. is "not-detected". Data are mean \pm SEM. * $P < 0.05$; *** $P < 0.001$.

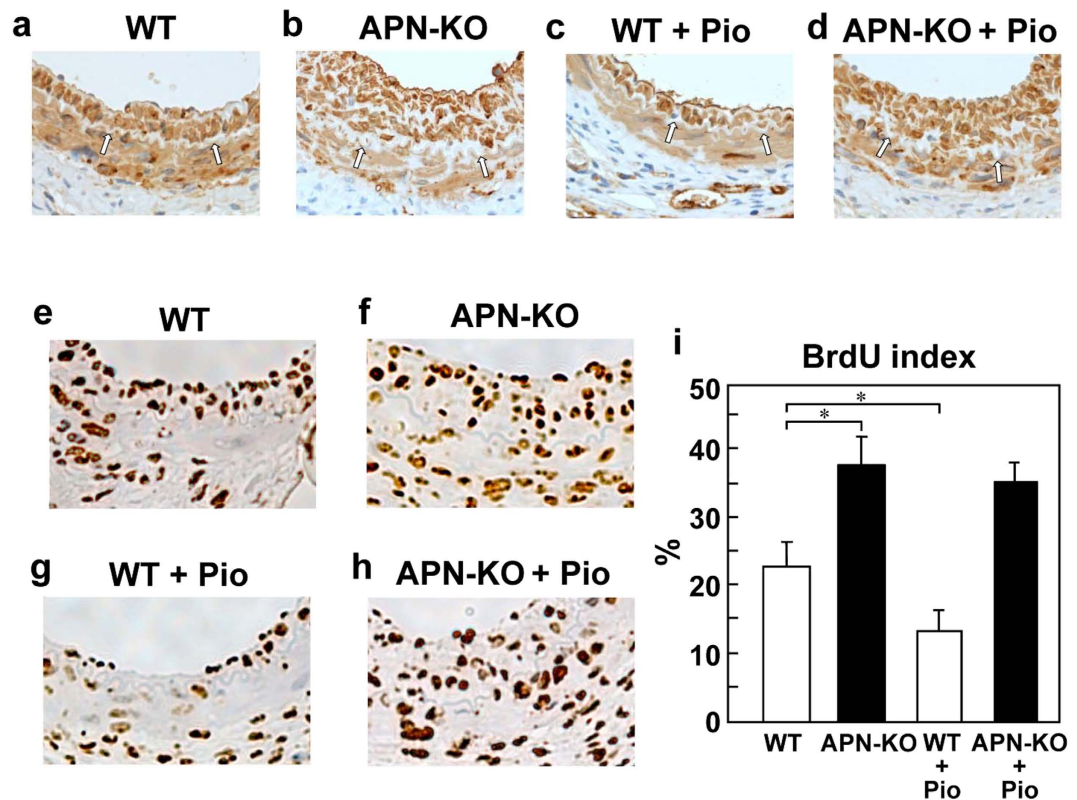


Figure 2. Pioglitazone treatment for 3 weeks suppressed cuff-induced VSMC proliferation in the WT mice, but not APN-KO mice. Representative immunohistochemical staining for alpha smooth muscle actin of injured vessels obtained from WT (a) APN-KO (b), WT+Pio (c) and APN-KO+Pio (d) mice after 3-weeks' treatment with pioglitazone. Representative BrdUrd staining for SMC proliferation (e–h) and ratio of the number of BrdUrd positive/BrdUrd- negative cells (i) in the arterial specimens obtained from the WT, APN-KO, WT+Pio and APN-KO+Pio mice after 3-weeks' treatment with pioglitazone (n = 5–6). Arrows show the internal elastic lamina. Data are mean \pm SEM. * $P < 0.05$.

positive staining for α -smooth muscle actin (Fig. 2a–d), as previously reported²⁷. These findings indicate that the cuff-induced neointimal formation is composed predominantly of VSMCs. We performed immunohistological analyses to assess the proliferation of VSMCs in the cuff-induced neointimal formation. The percentage of cells incorporating BrdU was significantly higher in the APN-KO mice than in the WT mice (Fig. 2e,f,i). Pioglitazone treatment for 3 weeks significantly reduced BrdU incorporation in the cuff-induced neointimal formation in the WT mice, but not in the APN-KO mice (Fig. 2g–i). These data suggest that the proliferation of the VSMCs in response to cuff injury was suppressed by pioglitazone treatment for 3 weeks through an adiponectin-dependent pathway.

Adiponectin suppressed PDGF-BB-induced VSMC proliferation via AdipoR1- and AdipoR2-mediated AMPK activation. To elucidate the adiponectin-dependent mechanisms underlying the suppression of VSMC proliferation by pioglitazone, we conducted an experiment using HASMCs. In previous studies in a rat carotid model, increase of PDGF-BB expression was demonstrated in the neointima formed after balloon injury, and a selective antagonist of PDGF-BB significantly reduced the neointimal formation^{28–30}. Thus, we observed adiponectin actions on PDGF-BB-induced VSMC proliferation in the HASMCs. In the BrdU incorporation assay, increased DNA synthesis induced by PDGF-BB was significantly suppressed by globular adiponectin, suggesting that adiponectin inhibits VSMC proliferation (Fig. 3a). Consistent with these data, the cell counting kit (CCK)-8 assay and WST-1 cell proliferation assay also revealed significant suppression by globular adiponectin of the enhanced cell viability induced by PDGF-BB (Supplementary Fig. S2a,b). Since adiponectin can activate AMPK in the liver and skeletal muscle²⁵, we investigated the phosphorylation of AMPK after stimulation with globular adiponectin in HASMCs or endothelium-denuded mouse aorta. Stimulation with globular adiponectin increased AMPK phosphorylation in both the HASMCs and endothelium-denuded mouse aorta (Fig. 3b,c). When the AMPK protein levels were reduced by transfection of siAMPK into the HASMCs, the PDGF-BB-stimulated VSMC proliferation was no longer suppressed (Fig. 3d and Supplementary Fig. S2c). These results suggest that AMPK activation by adiponectin suppressed PDGF-BB-induced VSMC proliferation in the HASMCs.

Since adiponectin is reported to activate AMPK via the adiponectin receptors, AdipoR1 and AdipoR2³¹, we investigated whether adiponectin also activated AMPK via AdipoR1 and AdipoR2 in the HASMCs. The expression of AdipoR1 mRNA was downregulated following transfection of AdipoR1 siRNA, whereas the AdipoR2

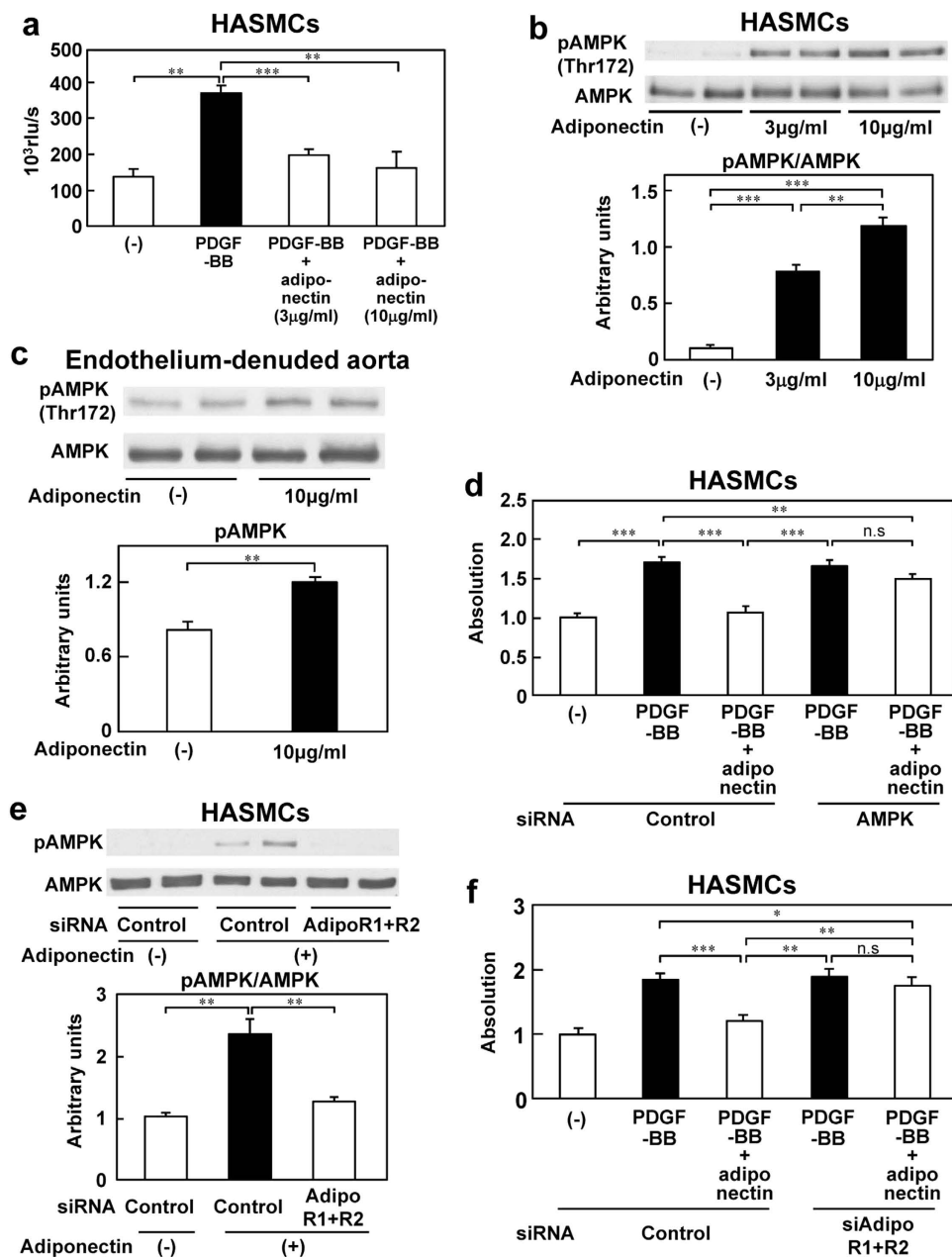


Figure 3. Adiponectin suppressed PDGF-BB induced HASMC proliferation through both AdipoR1- and AdipoR2-mediated AMPK activation. (a) Effect of globular adiponectin on PDGF-BB-induced BrdU incorporation in the HASMCs (n = 4–8). Phosphorylation of AMPK in the presence or absence of globular adiponectin in the HASMCs (b) (n = 4) and endothelium-denuded aorta in the WT mice (c) (n = 4). (d) Downregulation of AMPK by siAMPK abrogated the antiproliferative effect of globular adiponectin (n = 10). (e) Downregulation of both AdipoR1 and AdipoR2 completely abolished AMPK phosphorylation in the HASMCs (n = 4). (f) Downregulation of both AdipoR1 and AdipoR2 abrogated the antiproliferative effect of globular adiponectin in the HASMCs (n = 10). Data are mean \pm SEM. * P < 0.05; ** P < 0.01; *** P < 0.001.

mRNA levels remained unchanged (Supplementary Fig. S2d). Similarly, siAdipoR2 was used to reduce the expression levels of AdipoR2 mRNA without affecting the AdipoR1 mRNA expression levels (Supplementary Fig. S2d). Adiponectin-stimulated AMPK phosphorylation was partially disturbed by knockdown of AdipoR1 or AdipoR2 in the HASMCs (Supplementary Fig. S2e). Knockdown of both AdipoR1 and AdipoR2 almost completely suppressed the phosphorylation of AMPK by adiponectin (Fig. 3e and Supplementary Fig. S2f). Moreover, the effect of adiponectin of inhibiting PDGF-BB-stimulated VSMC proliferation was completely abrogated in the HASMCs (Fig. 3f). These data suggest that adiponectin suppresses PDGF-BB-stimulated VSMC proliferation through AdipoR1- and AdipoR2-mediated AMPK activation.

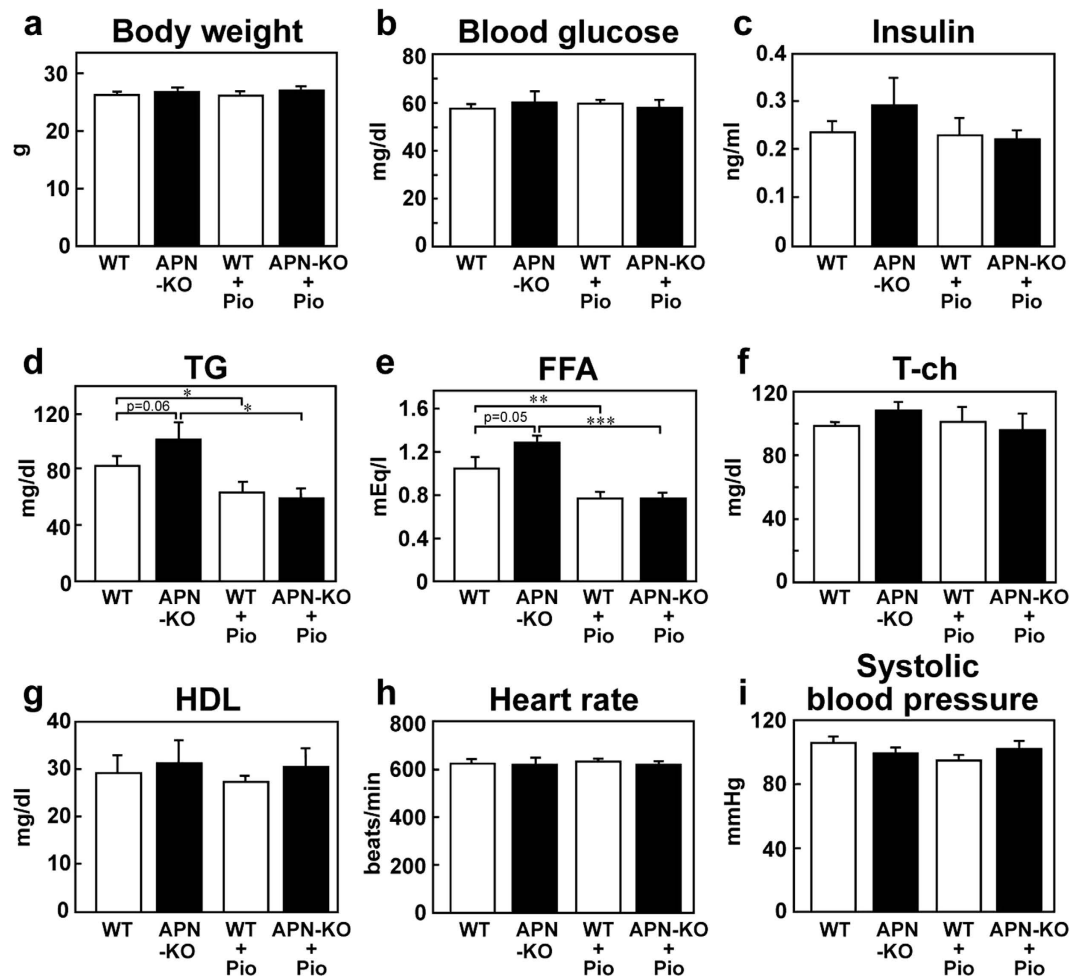


Figure 4. Pioglitazone treatment for 3 weeks improved the cardiovascular risk profile via an adiponectin-independent pathway (a) Body weight in the WT and APN-KO mice ($n = 6-8$). (b) Fasting blood glucose levels in the WT and APN-KO mice ($n = 6-8$). (c) Fasting plasma insulin levels in the WT and APN-KO mice ($n = 6-8$). (d) Fasting plasma triglyceride (TG) levels in the WT and APN-KO mice ($n = 6-8$). (e) Fasting plasma free fatty acid (FFA) levels in the WT and APN-KO mice ($n = 6-8$). (f) Fasting plasma total cholesterol (T-ch) levels in the WT and APN-KO mice ($n = 6-8$). (g) Fasting plasma high-density lipoprotein (HDL) levels in the WT and APN-KO mice ($n = 6-8$). (h) Heart rate in the WT and APN-KO mice ($n = 5-9$). (i) Systolic blood pressure in the WT and APN-KO mice ($n = 5-9$). Data are mean \pm SEM. * $P < 0.05$; ** $P < 0.01$; *** $P < 0.001$.

Pioglitazone treatment improved the cardiovascular risk profile in an adiponectin-independent manner. The body weight, blood glucose, plasma insulin level and plasma lipid profile were measured after 3 weeks of pioglitazone treatment. No significant differences were observed in the body weight, fasting blood glucose or plasma insulin levels among the four groups (Fig. 4a-c). Plasma triglyceride (TG) and free fatty acid (FFA) levels tended to be higher in the APN-KO mice than in the WT mice (Fig. 4d,e), as previously reported²⁰. Plasma TG and FFA levels in the APN-KO mice decreased to a degree similar to that obtained after 3 weeks of pioglitazone treatment in the WT mice (Fig. 4d,e), suggesting that these reductions occurred in an adiponectin-independent manner. No significant differences were observed in the total cholesterol (T-ch) or high-density lipoprotein (HDL) levels among the four groups (Fig. 4f,g). The heart rate and systolic blood pressure also did not differ among four groups after 3 weeks of pioglitazone treatment (Fig. 4h,i).

Pioglitazone treatment for 8 weeks significantly decreased cuff-induced neointimal formation in an adiponectin-independent manner. To investigate the effect of long-term pioglitazone treatment on cuff-induced neointimal formation, we administered pioglitazone to APN-KO and WT mice for 8 weeks. While the plasma total adiponectin levels significantly increased in the WT mice after 8 weeks of pioglitazone treatment to a similar degree as that at 3 weeks, no such increase was detectable in the APN-KO mice (Fig. 5a). Moreover, a similar degree of increase of the plasma HMW adiponectin levels was found after 8 weeks of pioglitazone treatment to that after 3 weeks of treatment in the WT mice, but not in the APN-KO mice (Supplementary Fig. S3). Cuff-induced increases of the intimal thickness and intimal/medial volume ratio were significantly higher in

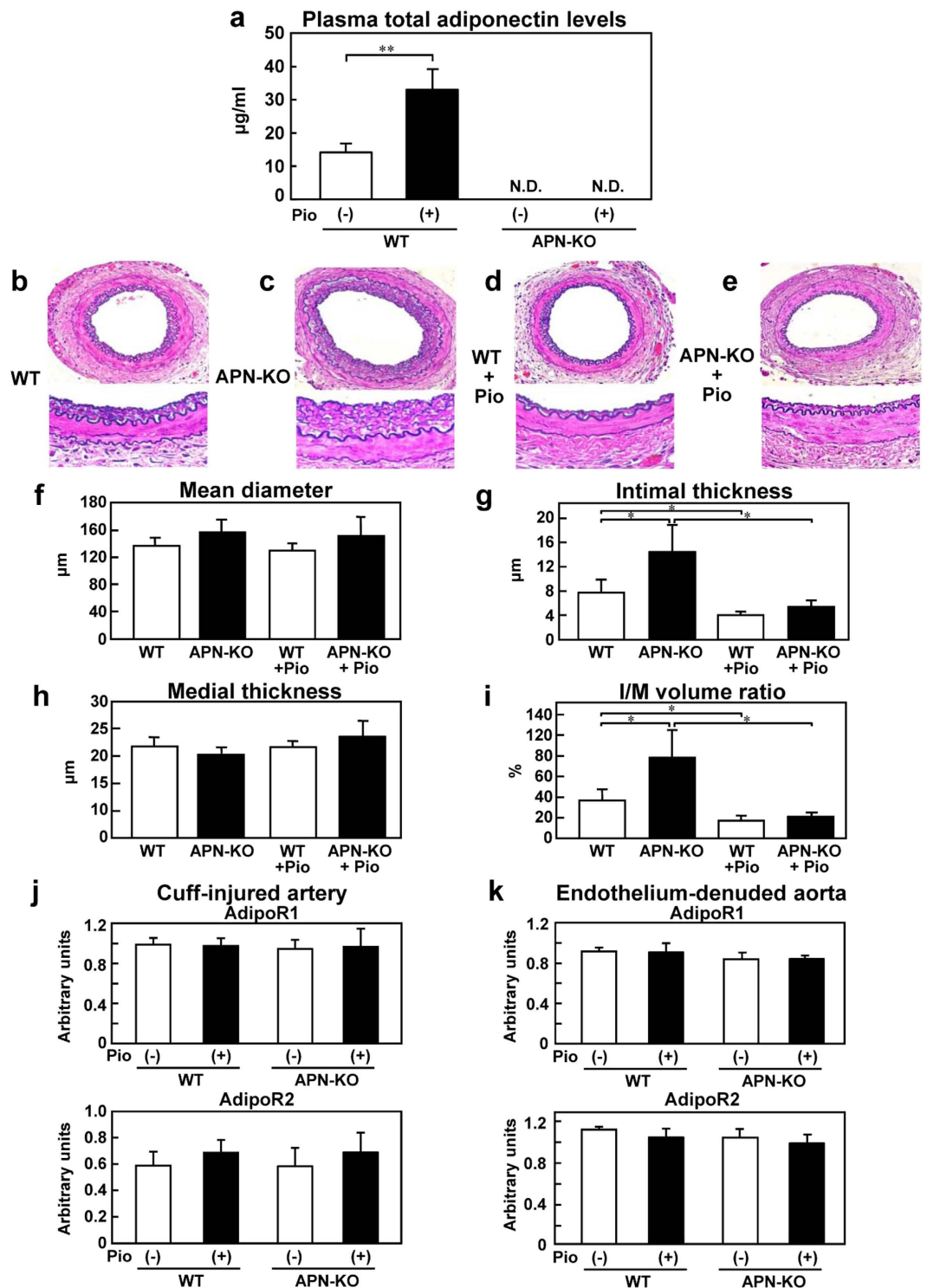


Figure 5. Pioglitazone treatment for 8 weeks inhibited cuff-induced neointimal formation in both WT and APN-KO mice. (a) Plasma total adiponectin levels after 8-weeks' treatment with pioglitazone in the WT and APN-KO mice ($n = 5$). Representative cuff-injured vessels from WT (b) APN-KO (c) WT+pioglitazone (Pio) (d) and APN-KO+Pio (e) mice after 8-weeks' treatment with pioglitazone (upper; $\times 40$, lower; $\times 400$). Morphometric analysis of the injured blood vessels; Mean diameter (f) Intimal thickness (g) Medial thickness (h) Intima-to-media (I/M) volume ratio (i) in response to 8-weeks' treatment with pioglitazone in the WT and APN-KO mice ($n = 9-12$). The expression levels of AdipoR1 and AdipoR2 in the cuff-injured artery (j) and endothelium-denuded aorta (k) in the WT and APN-KO mice ($n = 4-8$). N.D. is "not-detected". Data are mean \pm SEM. * $P < 0.05$; ** $P < 0.01$.

the APN-KO mice than in the WT mice (Fig. 5b,c,g,i). Interestingly, however, pioglitazone treatment for 8 weeks significantly reduced the cuff-induced increase of the intimal thickness and intimal/medial volume ratio in the APN-KO mice to a degree similar to that seen in the WT mice treated with pioglitazone for 8 weeks (Fig. 5d,e,g,i). There were no significant differences in the mean vessel diameter or medial thickness among the four groups (Fig. 5f,h). In contrast to the case after 3 weeks of pioglitazone treatment, no significant differences in either AdipoR1 expression or AdipoR2 expression in the cuffed artery or endothelium-denuded mouse aorta were observed among the four groups after 8 weeks of pioglitazone treatment (Fig. 5j,k). These data suggest that 8 weeks of pioglitazone treatment caused a significant decrease of cuff-induced neointimal formation via an adiponectin-independent mechanism.

Pioglitazone suppressed VSMC proliferation via regulation of cyclin B1 and cyclin D1 expression levels. Following 8-weeks' treatment with pioglitazone, similar to the observation after 3-weeks' treatment, the majority of the cells in the neointima of the cuff-injured vessels showed positive staining for α -smooth muscle actin (Supplementary Fig. S4a–d). Although the percentage of cells incorporating BrdU in the APN-KO mice was significantly higher than that in the WT mice, the percentage decreased significantly following 8 weeks of pioglitazone treatment to the same level as that in the pioglitazone-treated WT mice (Fig. 6a–e). These findings suggest that pioglitazone treatment is also capable of suppressing VSMC proliferation by an adiponectin-independent mechanism. Moreover, we investigated the expression levels of cyclin B1 and cyclin D1 in the cuff-injured artery in both the WT and APN-KO mice after 8 weeks of pioglitazone treatment. The expression levels of cyclin B1 and cyclin D1 in the cuffed artery were higher in the APN-KO mice than in the WT mice without pioglitazone treatment (Fig. 6f). After pioglitazone treatment for 8 weeks, these expression levels in the cuff-injured artery of the APN-KO mice decreased to levels similar to those seen in the WT mice treated with pioglitazone for 8 weeks (Fig. 6f). We investigated whether pioglitazone directly mediated VSMC proliferation by regulating the expression levels of cyclin B1 and cyclin D1. In the BrdU incorporation assay, increased DNA synthesis in the HASMCs induced by PDGF-BB was completely abolished by treatment with pioglitazone, suggesting that pioglitazone inhibits the proliferation of the VSMCs (Fig. 6g). Consistent with these data, the CCK-8 assay and WST-1 cell proliferation assay also revealed significant suppression by pioglitazone of the enhanced cell viability induced by PDGF-BB (Supplementary Fig. S4e,f). PDGF-BB upregulated the expressions of cyclin B1 and cyclin D1 mRNA, and the expression levels were reduced by pioglitazone treatment (Fig. 6h). On the other hand, the increased ERK phosphorylation and decreased expression levels of p21^{cip1} and p27^{Kip1} induced by PDGF-BB remained unchanged after pioglitazone treatment (Supplementary Fig. S4g–i). These data suggest that pioglitazone suppresses VSMC proliferation via regulating the expression levels of cyclin B1 and cyclin D1.

Pioglitazone treatment for 8 weeks improved the cardiovascular risk profile by an adiponectin-independent mechanism. Similar to the case after 3-weeks' pioglitazone treatment, we measured the body weight, blood glucose, plasma insulin levels and the plasma lipid profile after 8 weeks of pioglitazone treatment. No significant differences were observed in the body weight, blood glucose, plasma insulin or T-ch among the four groups (Fig. 7a–c,f). The increased plasma TG and FFA levels in the APN-KO mice reduced to a degree similar to that in the WT mice after 8 weeks of pioglitazone treatment (Fig. 7d,e). In addition to the reduction in the plasma levels of these parameters, significant increase of the plasma HDL levels was noted in both the WT and APN-KO mice after 8 weeks of pioglitazone treatment (Fig. 7g). Heart rate and systolic blood pressure did not differ among the four groups after 8 weeks of pioglitazone treatment (Fig. 7h,i). These data suggest that 8 weeks of pioglitazone treatment improved the cardiovascular risk profile via an adiponectin-independent mechanism.

Discussion

In this study, we demonstrated that pioglitazone treatment increased plasma adiponectin levels and AdipoR2 expression from the early phase of administration, resulting in the amelioration of cuff-induced neointimal formation through inhibition of VSMC proliferation. Adiponectin suppresses VSMC proliferation through both AdipoR1- and AdipoR2- AMPK pathways. In the late phase, on the other hand, the increased AdipoR2 expression seen in the early phase was blunted, and cuff-induced neointimal formation was similarly inhibited, in both the WT and APN-KO mice. Pioglitazone decreased VSMC proliferation via suppression of cyclin B1 and cyclin D1 mRNA expressions. These data suggest that the mechanism underlying the pioglitazone actions of inhibiting neointimal formation differs depending on the length of treatment. It acts via mainly an adiponectin-dependent pathway in the early phase of treatment but predominantly via an adiponectin-independent pathway in the later phase (Supplementary Fig. S5).

Increased plasma adiponectin following pioglitazone treatment for two weeks has been reported to be associated with improved insulin resistance and diabetes in ob/ob mice, but not in APN-KO/ob/ob mice³². Moreover, angiotensin II-induced cardiac hypertrophy and fibrosis improved following pioglitazone treatment for one week in WT mice, but not APN-KO mice³³. Adiponectin has been reported to promptly accumulate in damaged tissues, such as wire-injured vessels^{34,35}. These data suggest pioglitazone-induced suppression of neointimal formation mediated by adiponectin appears from the early phase of treatment. On the other hand, long-term pioglitazone treatment was associated with the inhibition of neointimal formation via an adiponectin-independent mechanisms. Although 8-weeks' treatment with pioglitazone increased the plasma adiponectin levels to the same degree as 3-weeks' treatment in the WT mice, cuff-induced neointimal formation improved in both the WT and APN-KO mice. The increased AdipoR2 expression observed after 3 weeks of pioglitazone treatment was blunted after 8-weeks' treatment in both the WT and APN-KO mice. A careful comparative study of WT and VSMC-specific PPAR γ -deficient mice revealed that although the plasma adiponectin levels appear to increase to

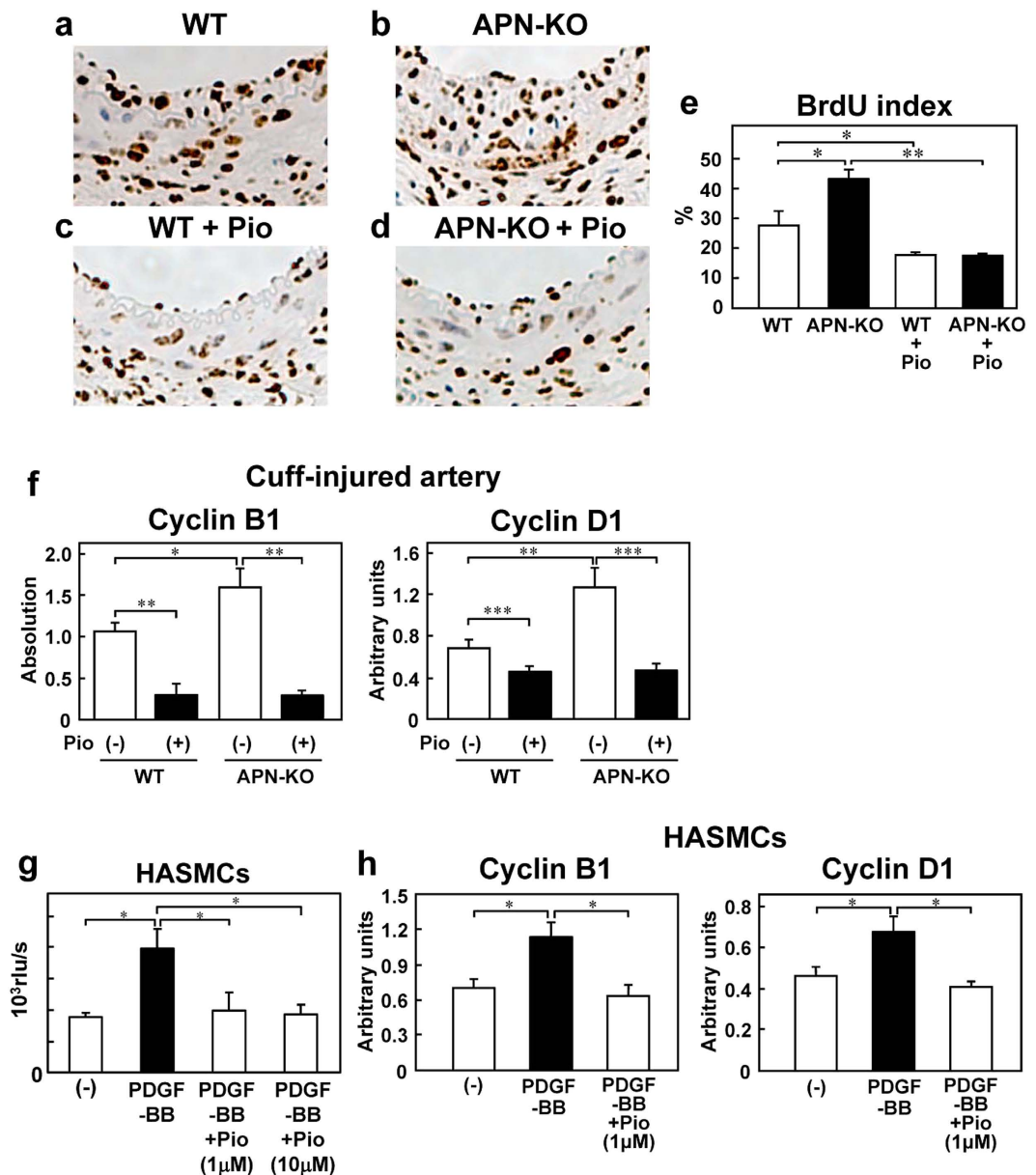


Figure 6. Pioglitazone treatment for 8 weeks suppressed cuff-induced VSMC proliferation in both WT and APN-KO mice. Representative BrdUrd staining for SMC proliferation (a–d) and ratio of the number of BrdUrd-positive/BrdUrd-negative cells (e) in the cuff-injured vessels obtained from WT, APN-KO, WT+Pio and APN-KO+Pio mice after 8-weeks' treatment with pioglitazone (n = 5–6). (f) Expression levels of cyclin B1 and cyclin D1 in the cuff-injured artery in the WT and APN-KO mice (n = 6–7). (g) Effect of pioglitazone on PDGF-BB-induced BrdU incorporation in the HASMCs (n = 4–8). (h) Pioglitazone reduced the expression levels of cyclin B1 and cyclin D1 after PDGF-BB stimulation in the HASMCs (n = 4). Data are mean ± SEM. * $P < 0.05$; ** $P < 0.01$; *** $P < 0.001$.

the same degree in these mice, pioglitazone administration for a relatively long period inhibited the progression of atherosclerosis in the WT mice, but not in VSMC-specific PPAR γ -deficient mice^{16,17}.

Full-length adiponectin has a collagen domain, which is directly capable of binding to PDGF-BB²² and attenuating PDGF β -receptor autophosphorylation, resulting in inhibition of PDGF-BB-induced VSMC proliferation^{22,36}. To investigate the effect of adiponectin on PDGF-BB-induced VSMC proliferation in the absence of direct binding with PDGF-BB and full-length adiponectin, we selected globular adiponectin to examine its effect on PDGF-BB-induced VSMC proliferation. Su *et al.* have reported that globular adiponectin inhibited PDGF-BB-induced mesangial cell proliferation without PDGF β -receptor autophosphorylation³⁷. Although T-cadherin, which has been identified as one of the adiponectin receptors, specifically binds to HMW adiponectin^{38,39}, both AdipoR1 and AdipoR2 can bind to globular adiponectin as well as full-length adiponectin²⁵. Thus, we could easily observe the action of adiponectin via the AdipoRs-AMPK pathway by using globular adiponectin, instead of full-length adiponectin.

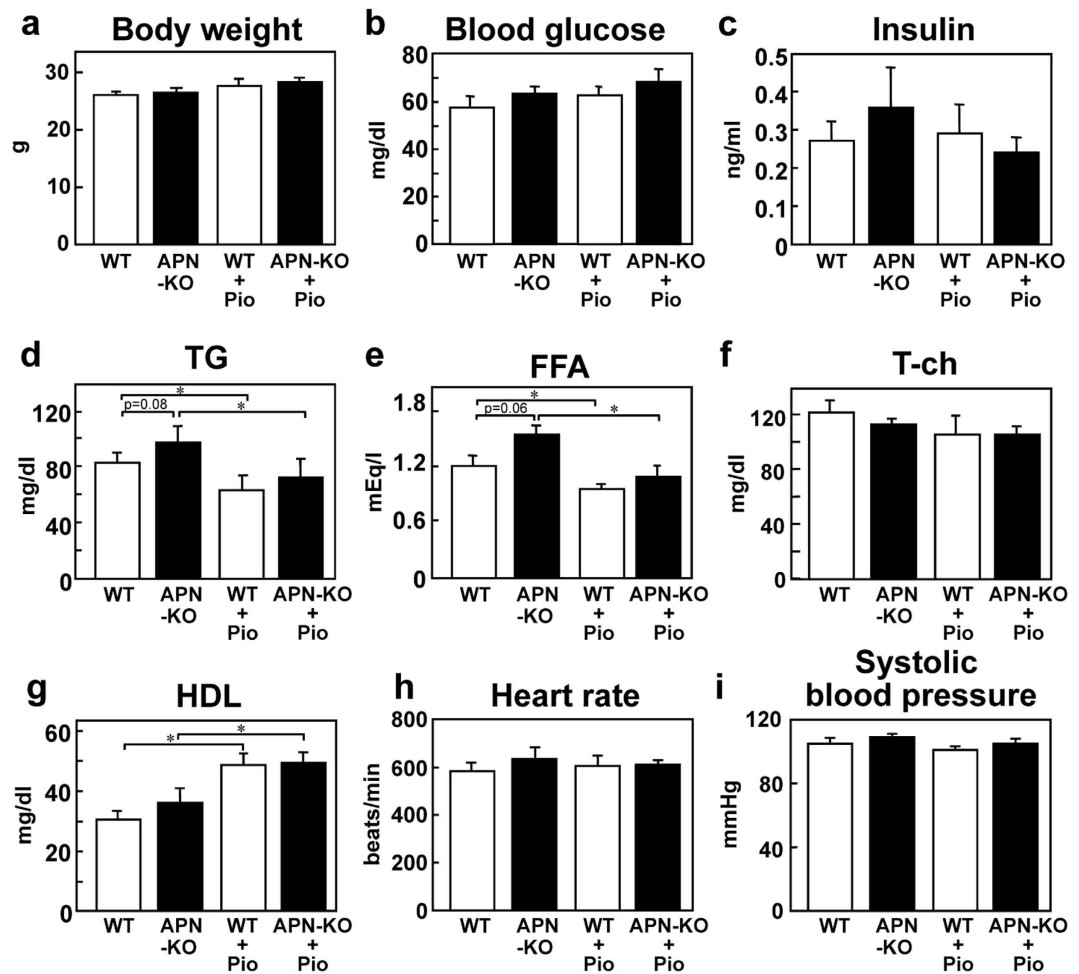


Figure 7. Pioglitazone treatment for 8 weeks improved the cardiovascular risk profile via an adiponectin-independent pathway (a) Body weight in the WT and APN-KO mice (n = 7–8). (b) Fasting blood glucose levels in the WT and APN-KO mice (n = 7–8). (c) Fasting plasma insulin levels in the WT and APN-KO mice (n = 7–8). (d) Fasting plasma triglyceride (TG) levels in the WT and APN-KO mice (n = 7–8). (e) Fasting plasma free fatty acid (FFA) levels in the WT and APN-KO mice (n = 7–8). (f) Fasting plasma total cholesterol (T-ch) levels in the WT and APN-KO mice (n = 7–8). (g) Fasting plasma high-density lipoprotein (HDL) levels in the WT and APN-KO mice (n = 7–8). (h) Heart rate in the WT and APN-KO mice (n = 5–6). (i) Systolic blood pressure in the WT and APN-KO mice (n = 5–6). Data are mean \pm SEM. * $P < 0.05$.

Pioglitazone activates PPAR γ , which is a key transcription factor for insulin sensitivity genes. VSMC-specific PPAR γ -deficient mice show accelerated atherosclerosis, which is not inhibited by pioglitazone administration¹⁷. Pioglitazone has been demonstrated to suppress cyclin B1 and D1 mRNA expressions via PPAR γ activation *in vitro*, resulting in the inhibition of VSMC proliferation¹⁸. On the other hand, pioglitazone was also shown to inhibit proliferation of VSMCs through the p38 MAPK-regulated cell cycle via a PPAR γ -independent pathway⁴⁰. TZDs inhibit Ang II-induced kruppel-like factor (KLF) 5 production, resulting in the suppression of cyclin D1 expression in the VSMCs via a PPAR γ -independent mechanism⁴¹. Thus, pioglitazone may inhibit the proliferation of VSMCs via both PPAR γ -dependent and PPAR γ -independent pathways.

Osman *et al.* demonstrated that treatment with 30 μ M pioglitazone inhibited PDGF-BB-induced VSMC proliferation by inhibiting the mTOR activity via an AMPK-dependent mechanism⁴². Following downregulation of AMPK by target-specific siRNA, 30 μ M pioglitazone inhibited ERK phosphorylation, thereby suppressing PDGF-BB-induced VSMC proliferation in an AMPK-independent manner. Moreover, both the AMPK-dependent suppression of the mTOR activity and AMPK-independent suppression of ERK phosphorylation occurred independently of PPAR γ expression⁴². On the other hand, we demonstrated that 1 μ M pioglitazone suppressed PDGF-BB-induced VSMC proliferation, although it had no effect on ERK phosphorylation (Fig. 6g and Supplementary Fig. S4g). It has been shown in a previous study that pioglitazone treatment at 1 μ M suppresses VSMC proliferation via PPAR γ activation¹⁸. These data suggest that the mechanisms of action of pioglitazone may differ depending on the dose; while at low concentrations, pioglitazone exerts its beneficial actions in a PPAR γ -dependent manner, at higher doses, it exerts its beneficial actions via PPAR γ -independent mechanisms.

Although no significant differences in the plasma HDL levels among the four study groups were observed after 3 weeks of pioglitazone treatment (Fig. 4g), 8 weeks of pioglitazone treatment was associated with increased

plasma HDL levels in both the WT and APN-KO mice (Fig. 7g). Consistent with these observations, a previous study showed that pioglitazone treatment for 4 weeks had no effect on the serum HDL levels in Wistar-Kyoto rats⁴³. On the other hand, Xing *et al.* demonstrated that pioglitazone treatment for 8 weeks increased the plasma HDL levels in Sprague-Dawley rats⁴⁴. Moreover, in a randomized clinical trial, pioglitazone treatment for 24 weeks was found to be associated with a decrease of the carotid intima-media thickness in type 2 diabetics, along with increase of the plasma HDL levels⁴⁵. Apolipoprotein (apo) A-I is produced in the liver and small intestine, and is one of the major constituents of the HDL-cholesterol fraction⁴⁶. The promoter region of apoA-I contains a peroxisome proliferator-responsive element (PPARE), and pioglitazone has been reported to increase apoA-I production by directly enhancing PPARE-dependent transcription⁴⁷. These data suggest that pioglitazone treatment, at least over the long term, increases the plasma HDL levels in both animal models and humans.

We could not demonstrate in this study whether long-term pioglitazone treatment exerted a stronger effect against neointimal formation than short-term pioglitazone treatment, because cuff-induced neointimal formation in WT mice was substantially inhibited by even short-term pioglitazone treatment. However, our results revealed that two pathways underlie the pioglitazone actions of inhibiting neointimal formation; an adiponectin-dependent pathway and an adiponectin-independent pathway. Pioglitazone may exert potent efficacy against neointimal formation through different mechanisms depending on the time course.

Materials and Methods

Animals. All animal experiment were conducted in accordance with the principles of the “Guide to the Care and Use of Experimental Animals” and were approved by the Animal Care Committee of the University of Tokyo. The APN-KO mice were generated on the original C57BL6/129sv hybrid background^{20,32}. We backcrossed APN-KO mice with C57BL6 more than seven times. All mice were maintained under a 12/12 hour light/dark cycle. Pioglitazone was administered to the mice by admixing it with food at a concentration of 0.02% (w/w) for 3 weeks starting at 17 weeks of age, or for 8 weeks starting at 12 weeks of age (Supplemental Fig. S6). The drug was kindly provided by Takeda Chemical Institute Co., Ltd (Kanagawa, Japan).

Cuff placement, tissue harvesting and morphometry. The mice were anesthetized by an intraperitoneal (IP) injection of 40–50 mg/kg of sodium pentobarbital. Then, an incision, about 7–10 mm in length, was made in the skin of the inguinal region under stereomicroscopic observation. The subcutaneous connective tissue was carefully removed to expose the femoral artery, followed by isolation of the femoral artery from the femoral vein by blunt dissection under stereomicroscopic observation. A polyethylene tube (inner diameter = 0.58 mm, length = 2 mm) was placed around the femoral artery. Finally, the surrounding tissue was straightened and the skin sutured. Pioglitazone administration was continued for 2 weeks after the cuff placement. Femoral arteries were then fixed *in situ* with 10% formalin and embedded in paraffin. Continuous cross-sections (5 μm) were then cut from one edge to the other of the cuffed portion. Morphometric analyses were performed on tissues stained for elastic fibers and with hematoxylin and eosin²⁷. The areas of the lumen, intima and media were measured in 10 cross sections using the image analyzer software, WinROOF (Mitani Corp), and then the volume ratio of the intima to media, intimal thickness, medial thickness and luminal diameter were calculated. The examiners of the sections were blinded to the genotype of the mice. Immunohistochemical staining was performed using anti-mouse α-smooth muscle actin (Abcam). Biotinylated secondary antibody and the ABC/DAB system (Vector) were used. Two weeks after cuff placement, the mice were anesthetized and saline was infused at a constant pressure of 100 mm Hg into the left ventricle. The cuff-injured femoral artery was immersed Trizol Reagent (Invitrogen) to extract RNA.

BrdUrd Staining. Following cuff placement, 100 μg/g of BrdUrd was administered intraperitoneally every 24 h until harvesting the femoral arteries. On the 14th day after vascular injury, the femoral arteries were perfusion-fixed in 10% formalin, harvested, and embedded in paraffin. After deparaffinization, parallel sections were immunostained with BrdUrd using a BrdUrd staining kit (Oncogene Research Products, Boston, MA). BrdUrd-labeled and -unlabeled SMCs in the neointima were counted in each section. The proliferation index was calculated by dividing the number of BrdUrd-labeled cells by the number of unlabeled cells.

Blood sample assay. Mice were denied access to food for 16 h before the measurements. 30-μl blood samples were collected from the tail vein in accordance with the guidelines for animal experiments of the University of Tokyo. Fasting blood glucose was measured with an automatic glucometer (Glutest Ace. Sanwa Chemical Co., Japan). Plasma levels of insulin (Morinaga Co., Ltd., Japan), triglyceride, total cholesterol, free fatty acids and high-density lipoprotein (Wako Pure Chemical Industries, Ltd., Japan) were assayed by enzymatic methods. Plasma total adiponectin levels (Otsuka Pharmaceutical Co., Ltd., Tokyo, Japan) and plasma HMW adiponectin levels (ALPCO Diagnostics., USA) were measured with ELISA kits.

Measurement of blood pressure and heart rate. Systolic blood pressure and pulse rate were measured with an automatic sphygmomanometer by the tail-cuff method in unanesthetized animals.

Western Blot Analysis. Cell and tissue samples were homogenized in ice-cold lysis buffer (25 mM Tris-HCl (pH 7.4), 10 mM sodium orthovanadate, 10 mM EDTA, 10 mM EGTA, 1% NP-40, 1 mM phenylmethylsulfonyl fluoride, and protease inhibitor cocktail). Identical amounts of protein were resolved by 10% SDS-PAGE and transferred to a Hybond-P PVDF transfer membrane (Amersham Biosciences). Bound antibodies were detected with HRP-conjugated secondary antibodies using ECL detection reagents (Amersham Biosciences). Anti-phospho-AMPK (Thr172), anti-pan-αAMPK (α1 and α2), anti-phospho-p42/44ERK, anti-ERK, and p21^{cip1} and p27^{kip1} antibodies were purchased from Cell Signaling.

Quantitative PCR. Total RNA was isolated from the cells and tissues with Trizol (Invitrogen), or an RNeasy Mini Kit (Qiagen Co., Germany), in accordance with the manufacturer's instructions. Less than one microgram of RNA was used for generating cDNA using random hexamers with QPCR master mix reagents (ABI). TaqMan quantitative PCR was then performed with the Applied Biosystems 7900HT Fast Realtime PCR system (Applied Biosystems) using TaqMan Gene Expression Assays or SYBR Green. TaqMan Gene Expression Assays used were as follows; AdipoR1, AdipoR2, CDKN1b. The primers used were as follows; Cyclin B1: 5'-CTGGGTCGGGAAGTCACTGGAAAC-3', 5'-GCAGCATCTTCTTGGGCACACA-3'; Cyclin D1: 5'-AGGCGGAGGAGAACAACAGATCA-3', 5'-AGAGGAAGCGTGTGAGGCGGTAGTA-3; GAPDH: 5'-AATGAAGGGTTCATTGATGG-3', 5'-AAGGTGAAGGTCGGAGTCAA-3'. The expression levels of each of the transcripts were normalized to the constitutive expression levels of β -actin and GAPDH mRNA.

siRNA transfection. Human aortic SMCs (HASMCs) and the smooth muscle cell growth medium (SmGM2) were purchased from Takara. For all the experiments, SMCs at passages 4–7 were used. HASMCs were seeded at 3×10^3 cells on to a 96-well dish; 24 hours after the plating, siControl (1.5 pmol; Santa Cruz), siAdipoR1 (1.5 pmol; Santa Cruz), siAdipoR2 (1.5 pmol; Santa Cruz), or siAMPK ($\alpha 1$ and $\alpha 2$) (1.5 pmol; Santa Cruz) diluted with Opti-MEM[®] was transfected into the cells with Lipofectamine RNAiMAX (Invitrogen). The cells were used for the assay 24 hours after the transfection.

Cell proliferation assay. For the cell counting assay, HASMCs were seeded at 3×10^3 cells on to a 96-well dish; 24 hours after the plating, the cells were serum-starved to render them quiescent by replacing the medium with DMEM containing 0.2% FBS. The quiescent SMCs were then preincubated with globular adiponectin (1 μ g/mL or 3 μ g/mL) or pioglitazone (1 μ M or 10 μ M) for 30 min. PDGF-BB (10 ng/mL) was added to stimulate the cells for 24 hours. These cells were incubated with 10 μ l of CCK (cell counting kit)-8 (DOJINDO) or WST-1 (Roche) solution for 2 hours before conducting the measurements. We measured the absorbance at 450 nm using a microplate reader. 10 μ l of BrdU (Roche) solution was added these cells simultaneously with PDGF-BB. We measured BrdU incorporation by chemiluminescent assay.

Endothelium-denuded aorta. Mice were sacrificed by an overdose of sodium pentobarbital. The thoracic aorta was gently excised, put in 0.2%FBS/DMEM, and the fat tissue around the aortic region was removed. The aorta was opened longitudinally with scissors, and the intimal surface of the vessels was delicately scrubbed with a cotton swab to remove the endothelium. The denuded aorta was stimulated with globular adiponectin 2 hours.

Statistical analysis. Values are expressed as means \pm S.E. Statistical analyses were performed by analysis of variance (ANOVA), and post hoc analysis was performed by the Turkey-Kramer method. P values of <0.05 were considered to indicate a statistically significant difference.

References

- Hofmann, C., Lorenz, K. & Colca, J. R. Glucose transport deficiency in diabetic animals is corrected by treatment with the oral antihyperglycemic agent pioglitazone. *Endocrinology* **129**, 1915–1925, doi: 10.1210/endo-129-4-1915 (1991).
- Kemnitz, J. W. *et al.* Pioglitazone increases insulin sensitivity, reduces blood glucose, insulin, and lipid levels, and lowers blood pressure, in obese, insulin-resistant rhesus monkeys. *Diabetes* **43**, 204–211 (1994).
- Miyazaki, Y. *et al.* Improved glycaemic control and enhanced insulin sensitivity in type 2 diabetic subjects treated with pioglitazone. *Diabetes Care* **24**, 710–719 (2001).
- Bajaj, M. *et al.* Pioglitazone reduces hepatic fat content and augments splanchnic glucose uptake in patients with type 2 diabetes. *Diabetes* **52**, 1364–1370 (2003).
- Dandona, P., Ghanim, H., Chaudhuri, A. & Mohanty, P. Thiazolidinediones-improving endothelial function and potential long-term benefits on cardiovascular disease in subjects with type 2 diabetes. *J. Diabetes Complications* **22**, 62–75, doi: 10.1016/j.jdiacomp.2006.10.009 (2008).
- Langenfeld, M. R. *et al.* Pioglitazone decreases carotid intima-media thickness independently of glycaemic control in patients with type 2 diabetes mellitus: results from a controlled randomized study. *Circulation* **111**, 2525–2531, doi: 10.1161/01.cir.0000165072.01672.21 (2005).
- Sidhu, J. S., Kaposzta, Z., Markus, H. S. & Kaski, J. C. Effect of rosiglitazone on common carotid intima-media thickness progression in coronary artery disease patients without diabetes mellitus. *Arterioscler. Thromb. Vasc. Biol.* **24**, 930–934, doi: 10.1161/01.atv.0000124890.40436.77 (2004).
- Bruemmer, D. & Law, R. E. Thiazolidinedione regulation of smooth muscle cell proliferation. *Am. J. Med.* **115** Suppl 8A, 87s–92s (2003).
- Shinohara, E. *et al.* Troglitazone suppresses intimal formation following balloon injury in insulin-resistant Zucker fatty rats. *Atherosclerosis* **136**, 275–279 (1998).
- Yoshimoto, T. *et al.* Vasculo-protective effects of insulin sensitizing agent pioglitazone in neointimal thickening and hypertensive vascular hypertrophy. *Atherosclerosis* **145**, 333–340 (1999).
- Riche, D. M., Valderrama, R. & Henyan, N. N. Thiazolidinediones and risk of repeat target vessel revascularization following percutaneous coronary intervention: A meta-analysis. *Diabetes Care* **30**, 384–388, doi: 10.2337/dc06-1854 (2007).
- Dormandy, J. A. *et al.* Secondary prevention of macrovascular events in patients with type 2 diabetes in the PROactive Study (PROspective pioglitazone Clinical Trial In macroVascular Events): a randomised controlled trial. *Lancet* **366**, 1279–1289, doi: 10.1016/s0140-6736(05)67528-9 (2005).
- Lehmann, J. M. *et al.* An antidiabetic thiazolidinedione is a high affinity ligand for peroxisome proliferator-activated receptor γ (PPAR γ). *J. Biol. Chem.* **270**, 12953–12956 (1995).
- Hsueh, W. A. & Law, R. E. PPAR γ and atherosclerosis: Effects on cell growth and movement. *Arterioscler. Thromb. Vasc. Biol.* **21**, 1891–1895 (2001).
- Law, R. E. *et al.* Expression and function of PPAR γ in rat and human vascular smooth muscle cells. *Circulation* **101**, 1311–1318 (2000).
- Hamblin, M. *et al.* Vascular smooth muscle cell peroxisome proliferator-activated receptor- γ mediates pioglitazone-reduced vascular lesion formation. *Arterioscler. Thromb. Vasc. Biol.* **31**, 352–359, doi: 10.1161/atvbaha.110.219006 (2011).
- Subramanian, V., Golledge, J., Ijaz, T., Bruemmer, D. & Daugherty, A. Pioglitazone-induced reductions in atherosclerosis occur via smooth muscle cell-specific interaction with PPAR γ . *Circ. Res.* **107**, 953–958, doi: 10.1161/circresaha.110.219089 (2010).

18. Wan, J. *et al.* Pioglitazone modulates the proliferation and apoptosis of vascular smooth muscle cells via peroxisome proliferators-activated receptor-gamma. *Diabetol. Metab. Syndr.* **6**, 101, doi: 10.1186/1758-5996-6-101 (2014).
19. Hui, X., Lam, K. S., Vanhoutte, P. M. & Xu, A. Adiponectin and cardiovascular health: an update. *Br. J. Pharmacol.* **165**, 574–590, doi: 10.1111/j.1476-5381.2011.01395.x (2012).
20. Kubota, N. *et al.* Disruption of adiponectin causes insulin resistance and neointimal formation. *J. Biol. Chem.* **277**, 25863–25866, doi: 10.1074/jbc.C200251200 (2002).
21. Matsuda, M. *et al.* Role of adiponectin in preventing vascular stenosis. The missing link of adipo-vascular axis. *J. Biol. Chem.* **277**, 37487–37491, doi: 10.1074/jbc.M206083200 (2002).
22. Wang, Y. *et al.* Adiponectin inhibits cell proliferation by interacting with several growth factors in an oligomerization-dependent manner. *J. Biol. Chem.* **280**, 18341–18347, doi: 10.1074/jbc.M501149200 (2005).
23. Frystyk, J. *et al.* Serum adiponectin is a predictor of coronary heart disease: A population-based 10-year follow-up study in elderly men. *J. Clin. Endocrinol. Metab.* **92**, 571–576, doi: 10.1210/jc.2006-1067 (2007).
24. Koenig, W., Khuseynova, N., Baumert, J., Meisinger, C. & Lowel, H. Serum concentrations of adiponectin and risk of type 2 diabetes mellitus and coronary heart disease in apparently healthy middle-aged men: Results from the 18-year follow-up of a large cohort from southern Germany. *J. Am. Coll. Cardiol.* **48**, 1369–1377, doi: 10.1016/j.jacc.2006.06.053 (2006).
25. Yamauchi, T. *et al.* Cloning of adiponectin receptors that mediate antidiabetic metabolic effects. *Nature* **423**, 762–769, doi: 10.1038/nature01705 (2003).
26. Shen, X., Li, H., Li, W., Wu, X. & Ding, X. Pioglitazone prevents hyperglycemia induced decrease of AdipoR1 and AdipoR2 in coronary arteries and coronary VSMCs. *Mol. Cell. Endocrinol.* **363**, 27–35, doi: 10.1016/j.mce.2012.07.005 (2012).
27. Kubota, T. *et al.* Lack of insulin receptor substrate-2 causes progressive neointima formation in response to vessel injury. *Circulation* **107**, 3073–3080, doi: 10.1161/01.cir.0000070937.52035.25 (2003).
28. Lindner, V., Giachelli, C. M., Schwartz, S. M. & Reidy, M. A. A subpopulation of smooth muscle cells in injured rat arteries expresses platelet-derived growth factor-B chain mRNA. *Circ. Res.* **76**, 951–957 (1995).
29. Ferns, G. A. *et al.* Inhibition of neointimal smooth muscle accumulation after angioplasty by an antibody to PDGF. *Science* **253**, 1129–1132 (1991).
30. Deguchi, J. *et al.* Targeting endogenous platelet-derived growth factor B-chain by adenovirus-mediated gene transfer potently inhibits *in vivo* smooth muscle proliferation after arterial injury. *Gene Ther.* **6**, 956–965, doi: 10.1038/sj.gt.3300918 (1999).
31. Kim, A. Y. *et al.* Adiponectin represses colon cancer cell proliferation via AdipoR1- and -R2-mediated AMPK activation. *Mol. Endocrinol.* **24**, 1441–1452, doi: 10.1210/me.2009-0498 (2010).
32. Kubota, N. *et al.* Pioglitazone ameliorates insulin resistance and diabetes by both Adiponectin-dependent and -independent pathways. *J. Biol. Chem.* **281**, 8748–8755, doi: 10.1074/jbc.M505649200 (2006).
33. Li, P. *et al.* Evidence for the importance of adiponectin in the cardioprotective effects of pioglitazone. *Hypertension* **55**, 69–75, doi: 10.1161/hypertensionaha.109.141655 (2010).
34. Okamoto, Y. *et al.* An adipocyte-derived plasma protein, adiponectin, adheres to injured vascular walls. *Horm. Metab. Res.* **32**, 47–50, doi: 10.1055/s-2007-978586 (2000).
35. Fujita, K. *et al.* Adiponectin protects against angiotensin II-induced cardiac fibrosis through activation of PPAR- α . *Arterioscler. Thromb. Vasc. Biol.* **28**, 863–870, doi: 10.1161/atvbaha.107.156687 (2008).
36. Arita, Y. *et al.* Adipocyte-derived plasma protein adiponectin acts as a platelet-derived growth factor-BB-binding protein and regulates growth factor-induced common postreceptor signal in vascular smooth muscle cell. *Circulation* **105**, 2893–2898 (2002).
37. Su, Y. X., Deng, H. C., Zhang, M. X., Long, J. & Peng, Z. G. Adiponectin inhibits PDGF-induced mesangial cell proliferation: Regulation of mammalian target of rapamycin-mediated survival pathway by adenosine 5-monophosphate-activated protein kinase. *Horm. Metab. Res.* **44**, 21–27, doi: 10.1055/s-0031-1295404 (2012).
38. Hug, C. *et al.* T-cadherin is a receptor for hexameric and high-molecular-weight forms of Acrp30/adiponectin. *Proc. Natl. Acad. Sci. USA* **101**, 10308–10313, doi: 10.1073/pnas.0403382101 (2004).
39. Takeuchi, T., Adachi, Y., Ohtsuki, Y. & Furihata, M. Adiponectin receptors, with special focus on the role of the third receptor, T-cadherin, in vascular disease. *Med. Mol. Morphol.* **40**, 115–120, doi: 10.1007/s00795-007-0364-9 (2007).
40. Li, L. *et al.* Pioglitazone inhibits homocysteine-induced migration of vascular smooth muscle cells through a peroxisome proliferator-activated receptor γ -independent mechanism. *Clin. Exp. Pharmacol. Physiol.* **35**, 1471–1476, doi: 10.1111/j.1440-1681.2008.05025.x (2008).
41. Liu, Y., Wen, J. K., Dong, L. H., Zheng, B. & Han, M. Kruppel-like factor (KLF) 5 mediates cyclin D1 expression and cell proliferation via interaction with c-Jun in Ang II-induced VSMCs. *Acta Pharmacol. Sin.* **31**, 10–18, doi: 10.1038/aps.2009.185 (2010).
42. Osman, I. & Segar, L. Pioglitazone, a PPAR γ agonist, attenuates PDGF-induced vascular smooth muscle cell proliferation through AMPK-dependent and AMPK-independent inhibition of mTOR/p70S6K and ERK signaling. *Biochem. Pharmacol.* **101**, 54–70, doi: 10.1016/j.bcp.2015.11.026 (2016).
43. Ishibashi, M. *et al.* Antiinflammatory and antiarteriosclerotic effects of pioglitazone. *Hypertension* **40**, 687–693 (2002).
44. Xing, Y., Ye, S., Chen, Y., Hu, W. & Chen, Y. Hydrochloride pioglitazone protects diabetic rats against podocyte injury through preserving glomerular podocalyxin expression. *Arq. Bras. Endocrinol. Metabol.* **58**, 630–639 (2014).
45. Mazzone, T. *et al.* Effect of pioglitazone compared with glimepiride on carotid intima-media thickness in type 2 diabetes: a randomized trial. *JAMA* **296**, 2572–2581, doi: 10.1001/jama.296.21.joc60158 (2006).
46. Paszty, C., Maeda, N., Verstuyft, J. & Rubin, E. M. Apolipoprotein AI transgene corrects apolipoprotein E deficiency-induced atherosclerosis in mice. *J. Clin. Invest.* **94**, 899–903, doi: 10.1172/jci117412 (1994).
47. Zhang, L. H., Kamanna, V. S., Ganji, S. H., Xiong, X. M. & Kashyap, M. L. Pioglitazone increases apolipoprotein A-I production by directly enhancing PPRE-dependent transcription in HepG2 cells. *J. Lipid Res.* **51**, 2211–2222, doi: 10.1194/jlr.M004481 (2010).

Acknowledgements

We thank Yrika Shiraishi, Namiko Okajima-Kasuga, Manami Takagi, Aymi Ito, Ayami Gouda, Michiko Tabara, Masatugu Takayasu and Masahiro Nakamaru for their technical assistance and care of the animals. This work was supported by a grant for CREST from the Japan Science and Technology Corporation, a grant for Promotion of Fundamental Studies in Health Science from the Organization for Pharmaceutical Safety and Research, a grant for TSBMI from the Ministry of Education, Culture, Sports, Science and Technology of Japan, a Grant-in-aid for Scientific Research (A) (16209030) and (A) (18209033) from the Ministry of Education, Culture, Sports, Science and Technology of Japan (to T. K.), and a Grant-in-aid for Scientific Research (C) (19591037) from the Ministry of Education, Culture, Sports, Science and Technology of Japan (to N. K.).

Author Contributions

T. Kubota performed experiments and data analysis; contributed to the experimental design; and wrote the manuscript. N.K. planned the experiments; and wrote the manuscript. H.S., performed experiments and data analysis; contributed to the experimental design. M.I., H.K., T.I. and K.T. performed experiments and data

analysis. M.M, Y.T., T. Kubota and K.U. contributed to experimental design and contributed to writing the manuscript. T. Kadowaki designed the experiments; wrote the manuscript; and obtained funding for the work.

Additional Information

Supplementary information accompanies this paper at <http://www.nature.com/srep>

Competing financial interests: The authors declare no competing financial interests.

How to cite this article: Kubota, T. *et al.* Pioglitazone Ameliorates Smooth Muscle Cell Proliferation in Cuff-Induced Neointimal Formation by Both Adiponectin-Dependent and -Independent Pathways. *Sci. Rep.* **6**, 34707; doi: 10.1038/srep34707 (2016).



This work is licensed under a Creative Commons Attribution 4.0 International License. The images or other third party material in this article are included in the article's Creative Commons license, unless indicated otherwise in the credit line; if the material is not included under the Creative Commons license, users will need to obtain permission from the license holder to reproduce the material. To view a copy of this license, visit <http://creativecommons.org/licenses/by/4.0/>

© The Author(s) 2016